

Human pluripotent stem cell-derived hepatocyte-like cells for hepatitis D virus studies

Huanting Chi^{1,2†}, Bingqian Qu^{3†§}, Angga Prawira³, Lars Maurer^{1,4}, Jungen Hu¹, Rebecca M. Fu¹, Florian A. Lemp^{3||}, Zhenfeng Zhang^{3¶}, Dirk Grimm^{2,4,5}, Xianfang Wu⁶, Stephan Urban^{2,3*‡}, and Viet Loan Dao Thi^{1,2*‡}

¹Schaller Research Group, Department of Infectious Diseases, Virology, University Hospital Heidelberg, Heidelberg, Germany; ²German Centre for Infection Research (DZIF), Partner Site Heidelberg, Heidelberg, Germany; ³Molecular Virology, Department of Infectious Diseases, University Hospital Heidelberg, Heidelberg, Germany; ⁴Department of Infectious Diseases, Virology, Section Viral Vector Technologies, University Hospital Heidelberg, Cluster of Excellence CellNetworks, BioQuant, Center for Integrative Infectious Diseases Research (CIID), Heidelberg, Germany; ⁵German Center for Cardiovascular Research (DZHK), Partner Site Heidelberg, Heidelberg, Germany; ⁶Infection Biology Program and Department of Cancer Biology, Lerner Research Institute, Cleveland Clinic Foundation, Cleveland, OH, USA.

14 Current address:

[§]Division of Veterinary Medicine, Paul-Ehrlich-Institut, Langen, Germany

IIVir Biotechnology, San Francisco, CA, USA

17 ¹School of Public Health and Emergency Management, School of Medicine, Southern University
18 of Science and Technology, Shenzhen, China

19 [†]equal contribution

20 [‡]equal contribution

21 *Corresponding authors: Stephan.Urban@med.uni-heidelberg.de and

22 VietLoan.DaoThi@med.uni-heidelberg.de

23

24 **Keywords:**

25 Hepatitis D virus, hepatitis B virus, human pluripotent stem cells, hepatocyte-like cells, adeno-
26 associated virus, antiviral treatment

27 Electronic word count:

28 **Number of figures and tables:** 6 figures, 1 table, 5 supplementary figures

29

30

81

37 **Abstract**

38 Current culture systems available for studying hepatitis D virus (HDV) are suboptimal. In this
39 study, we demonstrate that hepatocyte-like cells (HLCs) derived from human pluripotent stem
40 cells (hPSCs) are fully permissive to HDV infection across various tested genotypes. When co-
41 infected with the helper hepatitis B virus (HBV) or transduced to express the HBV envelope protein
42 HBsAg, HLCs effectively secrete infectious progeny virions. We also show that HLCs expressing
43 HBsAg support extracellular spread of HDV, thus providing a valuable platform for testing
44 available anti-HDV regimens. By challenging the cells along the differentiation with HDV infection,
45 we have identified CD63 as a potential HDV/HBV co-entry factor, which was rate-limiting HDV
46 infection in immature hepatocytes. Given their renewable source and the potential to derive
47 hPSCs from individual patients, we propose HLCs as a promising model for investigating HDV
48 biology. Our findings offer new insights into HDV infection and expand the repertoire of research
49 tools available for the development of therapeutic interventions.

50

51 **Teaser**

52 A human stem cell-derived hepatocyte culture model for hepatitis D virus studies

53 **Introduction**

54 Approximately 5% of chronic hepatitis B virus (HBV) carriers are co- or super-infected with
55 hepatitis D virus (HDV), resulting in an estimated 12 million chronic hepatitis D (CHD) patients
56 worldwide¹. However, a recent study suggests that these numbers probably represent an
57 underestimation of the true global burden of disease². HBV/HDV co-infection can cause the most
58 aggressive form of viral hepatitis, leading to an accelerated progression of liver dysfunction and
59 disease³.

60 HDV is a circular, single-stranded, negative-sense RNA virus that belongs to the
61 *Kolmioviridae* family. Based on their genome diversity, eight different HDV genotypes (GTs) have
62 been described, each showing distinct geographical distributions⁴. HDV-1 is the most prevalent
63 genotype and endemic worldwide, while infections with genotypes HDV-2 through -8 occur
64 regionally. HDV-2 infections are common in Southeast Asia, while the most diverged genotype
65 HDV-3 is exclusively prevalent in South America. HDV-4 is found in Japan and Taiwan and HDV-
66 5 through -8 infections are restricted to Africa⁵. Infection with the different GTs can lead to various
67 disease outcomes in the clinic: Compared to HDV-2, both HDV-1 and HDV-3 infections can lead
68 to severe hepatitis with more adverse patient outcomes⁶. Patients infected with HDV-4 usually
69 experience a mild course of liver disease. Patients with an HDV-5 infection appear to have a
70 preferable prognosis and respond better to pegylated interferon alpha (peg-IFN- α) treatment than
71 HDV-1 patients⁷. The clinical features of recently identified genotypes HDV-6 through -8 are less
72 characterized⁸.

73 HDV recruits HBV surface envelope proteins (HBsAg) for its progeny envelopment, which is
74 critical for HDV propagation and transmission⁴. Similar to HBV, HBsAg-enveloped HDV virions
75 enter hepatocytes through the interaction with the integral transmembrane protein receptor Na⁺-
76 taurocholate co-transporting polypeptide (NTCP)⁴. NTCP not only governs HDV liver tropism, but

77 also determines its species-specificity: only human and to a lesser extent mouse and rat NTCP
78 homologues support HDV entry, but not pig or macaque NTCP⁹⁻¹¹.

79 The HDV genome replicates in the nucleus using a double rolling circle mechanism,
80 generating intermediate antigenomic and genomic viral RNA strands¹². The mRNA transcribed
81 from the genomic RNA encodes only one open reading frame (ORF) which leads to the translation
82 of two proteins, the small (S-HDAg) and the large (L-HDAg) hepatitis delta antigen¹³. Editing of
83 the amber stop codon of the S-HDAg ORF in the antigenome by adenosine deaminase acting on
84 RNA 1 (ADAR1) elongates the reading frame by 19 to 20 codons, which drives the transition from
85 S- to L-HDAg synthesis¹⁴. Within the elongated terminus of L-HDAg, a recognition site for cellular
86 farnesyltransferase is modified and allows the switch towards virion assembly and release: while
87 S-HDAg facilitates, the farnesylated L-HDAg inhibits HDV genome replication. L-HDAg together
88 with the S-HDAg and the HDV genome initiates the formation of the ribonucleoprotein (RNP)
89 complex. The farnesyl group facilitates RNP attachment to the endoplasmic reticulum membrane
90 where HBsAg is located and new HDV progenies can be assembled¹⁹.

91 To date, fundamental aspects of HDV biology remain poorly understood, including molecular
92 details of its life cycle, the apparent genotype-dependent disease severity, and the underlying
93 mechanisms leading to accelerated liver dysfunction⁴. As a result, off-label peg-IFN- α was the
94 only available treatment for HDV infections for a long time. However, it cannot be used for all
95 patients, shows only limited efficiency, and often leads to significant side effects^{4,16}. Bulevirtide
96 (BLV, brand name Hepcludex, formerly known as Myrcludex B), has been recently granted
97 conditional marketing authorization by the European Medicines Agency (EMA)²². It is based on a
98 synthetic pre-S1-derived myristoylated peptide that specifically binds to NTCP and thus blocks
99 HBV and HDV entry. Recent real-world studies demonstrated that BLV as a monotherapy or in
100 combination with peg-IFN- α shows profound effects on HDV serum and liver RNA with possible
101 curative potential in a subset of patients¹⁹. The anti-HDV efficacy of farnesyltransferase inhibitor
102 Lonafarnib (LNF) which inhibits HDV progeny envelopment and therefore secretion, has been
103 demonstrated in phase 3 clinical trial when given in combination with either ritonavir or peg-IFN-
104 α ²⁰.

105 The gap in our understanding of HDV molecular biology and the lack of a curative treatment
106 is partially due to the restrictions of reproducible HDV cell culture systems that resemble the
107 physiological state of hepatocytes *in vivo*. Primary human hepatocytes (PHH) provide an
108 attractive model for HDV *in vitro* studies. However, their restricted availability, high donor-to-donor
109 variability, their difficulties in growing and maintaining them in culture for longer periods of time,
110 and the limited ability to manipulate them genetically impose severe limitations for reproducible
111 and high-throughput HDV studies²¹. Upon plating, PHH susceptibility to HDV infection drops
112 rapidly, due to the loss of hepatocyte polarization and NTCP expression²². On the other hand,
113 widely available and highly reproducible hepatoma cells can be only rendered permissive to HDV
114 infection upon induced or ectopic NTCP expression¹⁷. We have recently engineered a HepG2-
115 derived cell line that in addition to NTCP co-expresses the HBsAg, allowing us to study HDV
116 spread²³. However, hepatoma cells retain their transformed nature and members of the drug
117 metabolizing CYP450 family are only expressed to low levels in these cells²⁴. The human liver
118 bipotent progenitor cell line HepaRG becomes permissive to HDV infection upon differentiation
119 into hepatocytes²⁵. While differentiated HepaRGs cells retain many characteristics of PHHs, they
120 do not replicate all²⁶.

121 Recently, numerous protocols have been developed to differentiate human induced or
122 embryonic pluripotent stem cells (hiPSC/ESC) into hepatocyte-like cells (HLCs) (reviewed in²⁷).
123 HLCs resemble PHHs and better recapitulate physiological features, such as drug metabolism or
124 innate immune response, than hepatoma cells²⁸. In addition, stem cells represent a reproducible
125 and renewable resource that can be genetically manipulated. We and others have shown that
126 hESC- or iPSC-derived HLCs are suitable for HBV²⁹, hepatitis C virus (HCV)³⁰ and hepatitis E
127 virus (HEV)³¹ studies.

128 Here, we show that HLCs are readily permissive for HDV infection and replication of all
129 genotypes tested. We found that the co-infection with HBV or adeno-associated virus (AAV)-
130 mediated transduction of HBsAg in HLCs enabled HDV progeny assembly and release. We
131 demonstrate that HDV can spread extracellularly in HLCs which prompted us to evaluate the
132 efficacy of available anti-HDV regimens in HLCs. Finally, by challenging the cells at different
133 stages of HLC differentiation, we demonstrated the potential of this system to identify new host
134 factors that either promote or restrict HDV infection.

135

136 **Results**

137 *Hepatocyte-like cells (HLCs) are permissive for HDV infection in an NTCP-dependent manner
138 and can be co-infected with HBV*

139 Previous studies have demonstrated the utility of stem cell-derived HLCs for hepatotropic
140 virus infection, including HBV (reviewed in²⁷). Here, we analyzed whether HLCs are likewise
141 permissive to HDV infection.

142 We first used the HDV genotype (GT) 1 strain (JC126)³² to infect HLCs that we differentiated
143 from the human embryonic stem cell (hESC) line WA09 based on a previously optimized
144 protocol³³ (Fig. 1A). By the end of the differentiation, HLCs supported hepatocyte features
145 including indocyanine green uptake, glycogen synthesis, and the conversion of non-fluorogenic
146 carboxyfluorescein diacetate into fluorogenic carboxyfluorescein³³.

147 As shown in Suppl Fig. 1A & B, we detected increasing numbers of HDAg-positive HLCs in
148 an inoculum dose-dependent manner. HDV infection could be entirely blocked by pre-treating
149 HLCs with the inhibitor bulevirtide (BLV) (Fig. 1A), which is based on a synthetic lipopeptide that
150 mimics the receptor binding-site of HBV pre-S1 protein and binds to NTCP. Of note, while
151 differentiating the cells in the final maturation medium, we observed the formation of a second,
152 highly confluent HLC layer on top of the bottom HLC monolayer. Although we detected some
153 HDAg-positive cells in the bottom monolayer, we found the majority of HDV infections in the top
154 HLCs layer (Suppl Fig. 1A & Fig. 1A).

155 In order to evaluate the robustness of the system, we compared HDV infection of HLC with
156 conventional HDV culture systems. When applying the same HDV inoculum, HLCs were similarly
157 permissive to HDV infection (Fig. 1B) and replication (Fig. 1C) as differentiated HepaRG cells.
158 However, both HLCs and HepaRG cells were much less permissive than carcinoma-derived Huh7
159 cells ectopically expressing human NTCP (Huh7^{NTCP}, Fig. 1B & C and Suppl Fig. 1C).

160 Then, we assessed the possibility of further enhancing HDV infection by transducing HLCs
161 with recombinant, NTCP-encoding adeno-associated viruses (AAV) (Fig. 1D-F). We analyzed
162 endogenous and ectopic NTCP expression by microscopy using a fluorescently conjugated
163 peptide binding specifically to human NTCP (Fig. 1D). Unlike hepatoma cells, for which we and
164 others have observed a significant increase in HDV susceptibility upon NTCP replenishment¹⁷,

165 ectopic NTCP expression in HLCs enhanced HDV infection by only ~3-fold (Fig. 1E & F). This
166 indicated that in contrast to hepatoma cells, endogenous NTCP expression levels were not
167 majorly rate-limiting for productive HDV infection of HLCs. Of note, we also used the hESC line
168 RUES2 and the hiPSC line iPSC.C3A³⁴ (a kind gift from Stephen Duncan, MUSC) to generate
169 HLCs that were likewise permissive to HDV infection (data not shown), demonstrating the
170 reproducibility of the system.

171 Next, we analyzed HDV replication kinetics in HLCs by quantifying HDV genome copies over
172 time (Fig. 1G) up to 20 days post-infection (Suppl. Fig 1D). We observed a delayed onset of
173 replication by day 3 post-infection and a decrease in replication at later time points, which is similar
174 to HDV replication kinetics in other cell culture models, including primary human hepatocytes
175 (PHH)^{35,36}. We also infected HLCs with HDV GTs 3-8³⁷ and found that HLCs were permissive for
176 all tested genotypes (Fig. 1H and Suppl Fig. 1E).

177 Finally, we performed HBV genotype D and HDV GT1 co-infection of HLCs (Fig. 1I-L).
178 Although many infected HLCs were either HBV core (HBc) or HDV antigen (HDAg) single-
179 positive, we found ca. 25% of the infected cells to be double-positive for both HBc and HDAg,
180 suggesting productive co-infection with both viruses (Fig. 1J & K). Upon co-infection with HBV,
181 we detected infectious HDV progenies in the HLC culture medium showing that HLCs can fully
182 recapitulate the entire HDV life cycle (Fig. 1L).

183
184 *AAV transduction of HLCs with HBV surface antigens allows completion of the HDV life cycle in*
185 *HLCs in the absence of HBV infection*

186 It has been experimentally shown that HBsAg derived from naturally integrated HBV DNA
187 can support production of infectious HDV virions in the absence of active HBV replication^{38,39}.
188 Corroborating this, high HDV viremia has been detected in HDV/HBV carriers with low or
189 undetectable HBV levels⁴⁰, suggesting that HBV integrates are sufficient for expressing the HBV
190 envelope proteins.

191 To mimic this situation, we used a previously identified AAV capsid that transduces HLCs at
192 a high efficiency⁴¹ to express L-/M-/S-HBsAg in fully matured HLCs (HLCs^{HBsAg}, Fig. 2A). We
193 replaced the original promoter in the AAV transgene vector with the authentic HBV promoter in
194 order to gain the optimal ratio between the three envelope proteins enabling particle formation,
195 as we have shown before²³.

196 Six days post-HDV-infection, we detected secreted HBsAg in the supernatant of HLCs^{HBsAg}
197 (Fig. 2B) as well as HDV progenies, which were capable of initiating secondary infections in
198 Huh7^{NTCP} cells (Fig. 2C). HDV-infected HLCs^{HBsAg} continued to secrete both HBsAg and infectious
199 progenies until the end of the observation time, i.e., up to 21 days post-HDV infection.

200 In order to ensure that the secondary infections were not carry over events from the initial
201 HDV inoculum, we used the HBV/HDV entry inhibitor BLV and Lonafarnib (LNF), which prevents
202 prenylation of the C-terminal Cys211 residue in L-HDAg and thus the envelopment of infectious
203 HDV progenies⁴. LNF increased primary HDV infection of HLCs (Fig. 2D) in agreement with
204 previous results²³ but it fully blocked the assembly and release of infectious HDV progenies (Fig.
205 2E). As BLV already very potently blocked primary HDV infection of HLCs (Fig. 2D), we did not
206 observe any secondary infections in Huh7^{NTCP} (Fig. 2E). These data showed that HLCs can be
207 genetically engineered to express HBsAg allowing HDV to complete its life cycle.

208

209 *HDV extracellular spread in HLCs^{HBsAg} enables the evaluation of available antiviral HDV regimens*

210 HDV extracellular spread, which occurs efficiently *in vivo*, is difficult to replicate in currently
211 available *in vitro* models^{21,23}. Based on our observation that HDV progenies can be released from
212 HLCs^{HBsAg}, we analyzed whether they also supported HDV extracellular spread (Fig. 3). The
213 macromolecular crowding agent polyethylene glycol 8000 (PEG) is widely used to enhance HBV
214 and HDV infection in cell culture^{21,42,43} and we likewise used PEG 8000 for our primary HDV
215 infections of HLCs. To confirm that HDV extracellular spread without further addition of PEG is
216 possible in HLCs, we first confirmed that HLCs can be infected with HDV in the absence of PEG
217 (Suppl Fig. 2A & B).

218 Next, we transduced WA09 cells at their pluripotent stem cell stage with lentiviruses to
219 express ZsGreen and differentiated them to HLCs^{ZsGreen}. In parallel, we differentiated wild-type
220 WA09 cell and infected them with HDV and transduced them with AAVs to express HBsAg. We
221 then detached both HLC types and mixed the “recipient” HLCs^{ZsGreen} with “donor” HLCs^{HDV/HBsAg}.
222 Eight days later, we analyzed co-cultured donor and recipient HLCs for HDV infection by staining
223 against HDAg. As shown in Fig. 3A, we found HDAg-positive HLCs^{ZsGreen} in the vicinity of HDV-
224 infected donor HLCs. The treatment with BLV completely prevented infections of HLCs^{ZsGreen},
225 showing unequivocally that HDV extracellular spread had occurred in our HLC culture.

226 This prompted us to test the impact of available anti-HDV treatments on HDV spread in HLCs
227 (Fig. 3B). First, we infected HLCs with HDV to allow primary infection. The next day, we
228 transduced them with AAV-HBsAg. On the third day, we added the drugs to evaluate their impact
229 on the secondary infections, and accordingly, extracellular spread only. Since HLCs similar to
230 PHHs do not proliferate⁴⁴, we could exclude cell-division mediated spread.

231 Ten days post-infection, we observed that the treatment with a relatively high dose of 500 nM
232 BLV decreased the total HDV infection events compared to non-treated HLCs by roughly 50%
233 (Fig. 3C). In a dose-dependent manner, 10 nM BLV decreased total HDV infections by only ~25%.
234 Interestingly, the treatment with LNF, which prevents HDV assembly, did not have any impact on
235 the total number of HDV infections by day 10, but showed an effect when using the supernatant
236 to titer infectious progenies on Huh7^{NTCP} cells (Fig. 3D). This may be due to the observation that
237 LNF enhances primary infections (Fig. 2D) which is in agreement with reports by others^{23,45}. Of
238 note, the high dose of BLV completely abrogated secondary infection of Huh7^{NTCP} cells (Fig. 3D),
239 although some progenies must have been released from primary infected HLCs. This suggested
240 carry-over of BLV in the inoculum and highlights the advantage of using a culture system that
241 supports authentic and extracellular HDV spread.

242

243 *HDV susceptibility along HLC differentiation*

244 We finally wanted to determine the stage along the differentiation process at which HLCs
245 became susceptible to HDV infection. HLC differentiation is based on a five-step protocol
246 mimicking liver development with each step involving the exposure of the cells to different culture
247 media and growth factors: from hESC to definitive endoderm (DE), followed by hepatic
248 specification, then immature, and finally mature hepatocytes (Fig. 4A). We monitored the
249 differentiation progress by analyzing the expression of proteins (Fig. 4A) and transcript levels (Fig.
250 4B) of the immature hepatocyte marker alphafetoprotein (AFP), the mature hepatocyte marker
251 albumin (ALB), and NTCP. As soon as we cultured DE cells in the medium containing hepatocyte
252 growth factor to initiate hepatic specification, we observed a steep increase in AFP, ALB, and

253 NTCP expression levels (Fig. 4B). While AFP levels reached a plateau by day 13, ALB expression
254 only peaked by day 19 in the last culture medium, when the cells reached their final maturation
255 stage. Interestingly, NTCP was already expressed on the cell surface during the hepatic
256 specification stage but slightly decreased during the final maturation step.

257 Then, we infected the cells at either stem cell level (day 0), DE stage (day 5), or every second
258 day during the hepatocyte differentiation with HDV. 5 days post-infection we analyzed HDV
259 infections by quantifying HDV RNA copy numbers (Fig. 4C) and HDAg-positive cells (Fig. 4D) five
260 days post-infection. Neither hESC nor DE cells were susceptible to HDV infection (Fig. 4C & D).
261 Interestingly, when bypassing the cell entry step by delivering the HDV genome via transfection,
262 we found that hESCs were already capable of replicating HDV, as evidenced by the detection of
263 L-antigen in transfected cells (Suppl Fig. 3A).

264 We found that hepatic progenitors became susceptible to HDV infection as early as day 11
265 after starting the differentiation protocol, likely governed by the expression of NTCP. Interestingly,
266 immature hepatocytes at day 15 were less susceptible to HDV infection than the progenitors,
267 although they expressed NTCP on their surface. Then, we observed a second peak of HDV
268 infection, when the cells acquired a fully matured hepatocyte profile, as evidenced by the peak in
269 ALB expression at day 19 (Fig. 4B). Remarkably, NTCP expression was not further enhanced at
270 this point in time, indicating that other factors restricted HDV at the immature state. To identify the
271 exact day, we further refined and infected the cells with HDV every day between day 17 to 19
272 (Suppl Fig. 3B & C) of the differentiation protocol. We identified day 18 as the differentiation day
273 when cells became the most susceptible to HDV infection, roughly 2 days after we switched to
274 the final maturation medium. From day 19 on, HLCs became less susceptible to HDV infection,
275 likely due to a further decrease in NTCP expression (Fig. 4B) from the mature HLC stage on.
276

277 *Differential gene expression analysis reveals potential co- and restriction factors of HDV infection 278 in mature HLCs*

279 The enhanced permissiveness observed in matured HLCs by day 18 could be governed by
280 the upregulation of a host co-factor or the downregulation of a host restriction factor for HDV
281 infection. Thus, we compared the transcriptome profile of the cells between day 17 and day 18
282 (Fig. 5). Whole-transcriptome expression profiling and gene ontology (GO) term enrichment
283 analysis revealed up- or downregulation of genes enriched in many pathways, such as liver
284 development and regeneration (Fig. 5A). In agreement, individual markers of mature hepatocytes
285 such as ALB and PROX1 were upregulated, while markers of immature hepatocytes, such as
286 AFP and the stem cell marker SOX9, were downregulated by day 18 (Fig. 5B). FRZB is a negative
287 regulator of hepatocyte differentiation and was likewise downregulated by day 18.

288 We previously showed that stem cells express an intrinsic and protective subset of antiviral
289 genes (interferon stimulated genes, ISGs) and that they become downregulated throughout the
290 differentiation⁴⁶. In return, differentiated cells become more IFN-signaling-competent. In
291 agreement, we observed the downregulation of a subset of ISGs (Fig. 5C). Other factors such as
292 DDX58 and STAT1, which are critical for IFN induction and signaling, respectively (Fig. 5C), and
293 which rather play an antiviral role in mature hepatocytes, were upregulated.

294 Furthermore, the GO analysis revealed the upregulation of many genes that have been
295 previously described to be involved in the entry process of other viruses, including HBV (Fig. 3D).
296 Notably, genes encoding proteins that were found to interact with NTCP⁴⁷ as well as previously

297 described HBV and HDV co-entry factors were upregulated in mature HLCs by day 18. In addition,
298 numerous membrane receptors and co-factors involved in general viral entry were likewise
299 upregulated. We validated by RT-qPCR the upregulation of HBV entry co-factors along HLC
300 differentiation (Suppl Fig. 5A), such as caveolins⁴⁸ and LAMP1 as well as previously described
301 membrane receptors (Suppl Fig. 5B), such as EGFR⁴⁹, SCARB1⁵⁰, and LDLR⁵¹.
302

303 *CD63 is a potential co-factor of HDV entry and could be rate-limiting for infection of immature*
304 *hepatocytes.*

305 In order to identify a potential host factor that was expressed in mature HLCs and responsible
306 for enhanced HDV infection, we performed a small siRNA screen in Huh7^{NTCP} cells. We selected
307 siRNAs that target genes encoding membrane receptors and co-factors of viral entry and that
308 were upregulated in mature HLCs as revealed by the transcriptome analysis (Fig. 5D). As positive
309 controls, we also employed siRNAs targeting NTCP as well as the HDAg-coding region in the
310 HDV RNA genome.

311 As shown in Fig. 6A, the downregulation of several genes reduced HDV infection by up to
312 80% compared to the transfection with a non-target (nt) control siRNA. We selected the top four
313 candidate genes for further validation (Fig. 6B): the poliovirus receptor (PVR), CD63, as well as
314 integrins beta 1 (ITGB1) and alpha 2 which can form a functional ITGB1/A2 heterodimer. We
315 confirmed the downregulation of these genes by western blot analysis (Suppl Fig. 5A) and their
316 impact on HDV infection of Huh7^{NTCP} cells (Fig. 6B). However, the downregulation of PVR and
317 ITGA2 had a pronounced effect on cell attachment and cell viability (Fig. 6C). Since the
318 downregulation of CD63 decreased HDV infection by up to 50% in the absence of any effect on
319 either surface NTCP expression (Suppl Fig. 5B) or cell viability (Fig. 6C), we decided to follow up
320 on this host factor.

321 Next, we wanted to study whether CD63 plays a role in either the early steps of the HDV life
322 cycle, including cell entry, or at later steps, such as genome replication. Thus, we also delivered
323 the CD63 targeting siRNA one day after HDV infection of Huh7^{NTCP} cells (Fig. 6D). Only when
324 CD63 was downregulated before (Fig. 6A & B) but not after HDV infection, we observed a
325 significant reduction, suggesting that CD63 plays a role during the early steps of HDV infection,
326 but not replication. Since HBV shares the envelope glycoproteins with HDV, we also wanted to
327 analyze whether CD63 could play a role during HBV infection. As shown in Fig. 6E, although
328 CD63 downregulation had a significant effect on HBV infection, it affected it to a much lower extent
329 than HDV infection.

330 When analyzing CD63 expression along HLC differentiation, we found a distinct upregulation
331 in mature HLCs as compared to immature HLCs, on the transcript and protein level (Fig. 6F & G).
332 Interestingly, we also found that CD63 appeared to be less glycosylated in immature hepatocytes
333 as compared to mature hepatocytes (Fig. 6G), mirroring observations made in immature and
334 mature dendritic cells by others⁵². As described above and as shown in Fig. 1A and Suppl Fig.
335 1A, we observed throughout our experiments that HDV seemed to preferentially infect the highly
336 confluent, second layer of HLCs on top of the monolayer of HLCs at the bottom. By confocal
337 microscopy analysis, we indeed found that CD63 was more highly expressed in the top HLCs
338 layer (Fig. 6H & I) as compared to the lower HLC level (Fig. 6H & J).

339 We then wanted to rescue CD63 expression at the different hepatocyte maturation stages.
340 To this end, we AAV-transduced the cells at days 8, 13, and 17 of the differentiation protocol and

341 infected them with HDV at each time point two days later (Fig. 6K). Ectopic CD63 expression led
342 to a stronger, at least 2-fold increased HDV infection in immature hepatocytes but only to a 1.2-
343 fold increase in mature hepatocytes, showing that CD63 could be a rate-limiting factor for HDV-
344 infection of immature hepatocytes. Future studies shall provide a more mechanistic understanding
345 on how CD63 may be involved in HDV entry. Here, we provided a guideline of how stem cell
346 differentiation culture systems can be used as a platform for the identification of novel co-factors
347 for virus infection.

348

349 **Discussion**

350 Historically, studies of human hepatotropic viruses were hampered by the lack of
351 physiologically relevant hepatic cell culture models. Likewise, for HDV studies, the scarceness of
352 reproducible cell culture systems that resemble the physiological status of hepatocytes *in vivo*,
353 has hampered our progress in understanding important aspects of HDV biology. Previous studies
354 by us and others have shown the advantages of hPSC-derived HLCs for HBV, HCV, and HEV
355 investigations^{29,31,53}. Here, we demonstrated the applicability of HLCs for HDV studies.

356 *HLCs to study the entire life cycle of HDV and HBV/HDV co-infections*

357 We found that HLCs were readily permissive for HDV and HBV infection and that the ectopic
358 NTCP expression under a foreign promoter did not dramatically increase HDV infection. These
359 results are in stark contrast to hepatoma cells¹⁷ and highlight the authenticity of HLCs. Thus, HLCs
360 enable HDV infection studies under the physiological regulation of NTCP expression, which can
361 depend on bile acid concentrations, inflammatory cytokines, and others (reviewed in⁵⁴).

362 During the work on this manuscript, a study by Lange and colleagues⁴⁵ used HLCs to study
363 the innate immune responses to HDV mono-infection. Here, in contrast, we studied HDV biology
364 in the context of its helper virus. By either co-infecting with HBV or by genetically manipulating
365 HLCs to express HBsAg, we detected infectious HDV progenies in the HLC culture medium
366 showing that HLCs can recapitulate the entire HDV life cycle and even extracellular HDV spread.

367 Both *de novo* infection and cell division-mediated spread contributes to HDV persistence in
368 CHD patients⁵⁵. We have previously shown that HDV spreads in hepatoma cells upon cell division
369 and that it was highly dependent on the innate immune competence of the respective cell line
370 used⁵⁶. However, HDV extracellular spread is difficult to replicate in available *in vitro* models. On
371 the one hand, rapid de-differentiation and rapid decrease of NTCP expression after seeding
372 heavily restrict the use of PHHs for HDV spread studies²². On the other hand, hepatoma cells
373 ectopically expressing NTCP and HBsAg only poorly support extracellular spread, as shown in
374 our recent study²³. Here, we showed that HLCs support efficient extracellular HDV spread and
375 thus provide a physiologically relevant, reproducible, and non-proliferative cell model to study the
376 underlying determinants.

377

378 *HBsAg-HLCs for anti-HDV treatment evaluation*

379 HLCs express members of the CYP450 family and their drug responsiveness correlates with
380 those of PHHs⁵⁷. Therefore, numerous previous studies have proposed HLCs as a platform for
381 drug toxicity⁵⁸ and drug evaluation studies²⁸. In addition, owing to the self-renewal of stem cells,
382 HLCs can be easily upscaled and used for high-throughput drug screens⁵⁹. Finally, patient-
383 specific iPSCs can be generated from clinically relevant individuals to create personalized disease
384 and drug evaluation models.

385 Since HLCs^{HBsAg} supported extracellular HDV spread, we used them to test the currently
386 available drugs specifically developed to treat HDV infections. First, we confirmed that BLV
387 completely blocked HDV entry into HLCs. In contrast, the application of LNF led to more
388 detectable primary HDV infections, which may be related to intra-hepatocellular accumulation of
389 non-farnesylated and therefore non-inhibitory L-HDAg²³. As a result, we observed no significant
390 variation in total HDV infections after the treatment of LNF in our HLC spread assay. Only when
391 titrating HDV progenies separately and analyzing secondary infections, we could observe the
392 effect of LNF. Our findings highlight the advantage of studying the potency of drugs in a system
393 that faithfully recapitulates spread, especially since the currently available and specific anti-HDV
394 regimens target virus entry and assembly.
395

396 *Challenging HLCs along their differentiation revealed CD63 as a potential HDV/HBV entry factor*

397 To our surprise, NTCP was expressed very early during HLC differentiation which mimics
398 liver development. This early expression of NTCP rendered hepatic progenitors susceptible to
399 HDV infection, aligning with previous studies that showed non-hepatic cell lines becoming
400 susceptible to HDV infection upon ectopic NTCP expression¹¹. In agreement, we found stem cells
401 to be already capable of replicating the HDV genome when delivered through transfection,
402 bypassing the entry step, which is consistent with the findings by Lange *et al.*⁴⁵

403 Surprisingly, we discovered that fully matured HLCs at day 18 of differentiation exhibited a
404 higher susceptibility to HDV infection compared to less mature cells. This suggested the presence
405 of one or several hepatocyte-specific co-factors that facilitated HDV entry or replication. We ruled
406 out NTCP as the responsible determinant, as its expression was slightly decreased in fully
407 matured hepatocytes.

408 Our subsequent analysis using a small siRNA screen targeting selected genes from the
409 transcriptome analysis, revealed CD63 as a potential HBV and HDV entry factor. CD63 seemed
410 to be rate-limiting for HDV infection of immature hepatocytes which was alleviated by ectopic
411 CD63 expression. While CD63 is most prominently known for its role in exosomal egress and has
412 been reported to be involved in HBV assembly and egress⁶⁰, it is also a critical component of late
413 endosomes and facilitates vesicular trafficking through endosomal pathways⁶¹. As such, it has
414 been shown to be involved in the entry of other viruses^{62,63}.

415 It is important to note that CD63 is likely not the only factor governing enhanced infection of
416 mature HLCs, and future research should aim to identify and confirm such other factors. In
417 addition, further mechanistic studies will be needed to confirm and elucidate the role of CD63 in
418 HBV/HDV entry. In this study, we demonstrated how challenging cells along the stem cell
419 differentiation process can be a dynamic platform for discovering new host factors for virus
420 infection.

421 *Limitations of using HLCs for HDV infection studies*

422 While we have shown that HLCs support HDV infection, their susceptibility remained inferior
423 to the infection of hepatoma cells overexpressing NTCP, potentially due to their immature nature.
424 In addition, we observed that HDV preferentially infected the top layer of HLCs but not the bottom
425 layer. While we found a potential correlative expression with CD63, future studies shall identify
426 other critical co-factors for HDV infection being absent or potential restriction factors being present
427 in the different HLC populations. Comparing the genetic landscape between the two populations

429 could potentially lead to the identification of such factors. These factors could then be genetically
430 modified by lentiviral or AAV transduction, as we have done in this study, to yield highly permissive
431 HLCs.

432 Generally, stem cell culture and their differentiation remain expensive and time-consuming.
433 In the absence of a deep understanding of the molecular mechanism of liver development and
434 regeneration^{64,65}, a broad range of HLC differentiation protocols have been published for different
435 applications. A better understanding of liver development is needed and shall lead to the
436 development of more robust and potentially commercially available HLC differentiation kits in the
437 future. This should make the system available to all researchers in the field with the overarching
438 goal of advancing molecular HDV studies and developing curative and alternative therapies for
439 chronic HDV patients.

440

441 **Materials and methods**

442 *Reagents and antibodies*

443 The following antibodies were used for immunofluorescence staining or western blot analysis:
444 monoclonal mouse/human anti-HDAg³⁷ (1:3000, FD3A7; available through Absolute Antibody)
445 and rabbit anti-HBcAg antibody⁶⁶ (1:1000, H363) were generated in-house. Human anti-HBsAg
446 (1:1000, HBc34) was a kind gift from Davide Corti, Humabs BioMed. Rabbit anti-FoxA2 (1:400)
447 was purchased from Cell Signaling, mouse anti-AFP (1:1000) from Sigma-Aldrich, mouse anti-
448 ALB (1:1000) from Cedarlane and mouse anti-CD63 from SANTA CRUZ BIOTECHNOLOGY
449 (1:400). Alexa Fluor 488/568 anti-mouse (1:1000), Alexa Fluor 488 anti-human (1:1000), and
450 Alexa Fluor 488/568 anti-rabbit (1:1000) antibodies were purchased from Invitrogen. Antibodies
451 for western blot: mouse anti-CD63 (1:1000) was purchased from Invitrogen, rabbit anti-PVR
452 (1:1000) from Sigma-Aldrich, mouse anti-ITG β 1 (1:1000) from Santa Cruz and rabbit anti-ITG α 2
453 (1:1000) from Abcam. Lonafarnib was purchased from Selleckchem.

454

455 *Standard cell culture*

456 The human hepatoma cell line Huh7^{NTCP} and HepG2^{NTCP} ectopically expressing human NTCP
457 was generated previously⁶⁶. Huh7^{NTCP} and HepG2^{NTCP} cells were cultured in Dulbecco's modified
458 Eagle medium (DMEM, Gibco) supplemented with 10% advanced fetal bovine serum (FBS,
459 Capricorn) and 2 μ g/mL puromycin (InvivoGen). For AAV production, HEK-293T cells were
460 cultured in DMEM (Gibco), supplemented with 10% fetal bovine serum and 1% penicillin-
461 streptomycin (Gibco).

462

463 *Generation of human pluripotent stem cell-derived hepatocyte-like cells (HLCs)*

464 The use of human embryonic stem cells (hESC) for this work was approved by the German
465 Central Ethics Committee for Stem Cell Research (Robert Koch Institute, AZ: 3.04.02/0179). The
466 hESC line WA09 (WiCell) was cultured in mTeSR1 medium (STEMCELL Technologies) on
467 Matrigel (Corning) coated plates. WA09 cells were differentiated to definitive endoderm (DE)
468 using the STEMdiffTM Definitive Endoderm Kit (STEMCELL Technologies) according to the
469 manufacturer's protocol. To induce hepatic differentiation, DE cells were differentiated in the basal
470 medium consisting of CTSTM KnockOutTM DMEM/F12 (Gibco), 10% KnockOut Serum
471 Replacement (KOSR, Gibco), 1% MEM solution of non-essential amino acids (NEAA, Gibco), 1%
472 GlutaMAX supplement (Gibco), and 1% penicillin-streptomycin (Gibco), supplemented with

473 human hepatocyte growth factor (HGF, Prepotech), DMSO (Sigma-Aldrich), and dexamethasone
474 (Sigma) as previously described³³. For final maturation, HLCs were cultured in the Hepatocyte
475 Culture Medium BulletKit™ (HCM, Lonza) supplemented with 20 ng/mL of recombinant human
476 oncostatin M (OSM, R&D systems). For the co-culture experiment, WA09 cells were transduced
477 with lentivirus to express ZsGreen and selected with 1 µg/mL puromycin as described⁶⁷ prior to
478 HLC differentiation.

479

480 *HBV and HDV production and infection*

481 HBV (GT D) virus was produced from the HepF19 cell line as previously described⁶⁸. HDV
482 virus was produced as previously described²³. In brief, virus was collected from supernatants from
483 Huh7 cells co-transfected with plasmids pJC126³² (HDV GT1, kindly provided by John Taylor, Fox
484 Chase Cancer Center) and pT7HB2.7⁶⁹ (hepatitis B virus genotype D envelope proteins, kindly
485 provided by Camille Sureau, Institut National de la Transfusion Sanguine; accession number:
486 MN645906) and purified by heparin affinity chromatography. HDV virus stocks of GT1 Ethiopia
487 and 3-8 were produced as previously described³⁷.

488 HLCs were infected at day 18 of the differentiation protocol at an MOI of 5 infectious units
489 (IU) in the presence of 4% polyethylene glycol 8000 (PEG, Sigma-Aldrich) and 1.5% DMSO
490 (Sigma-Aldrich). 16 to 24 h later, the inoculum was removed and HLCs were washed twice with
491 Dulbecco's Phosphate Buffered Saline (DPBS) before replenishing with fresh culture medium
492 supplemented with 1.5% DMSO. Medium was exchanged every two days until the end of the
493 experiment.

494 For the secondary infection, 1x10⁵ Huh7^{NTCP} cells were seeded in 24-well plates and
495 inoculated with approximately one fifth of the culture supernatant from HDV-infected HLCs in
496 DMEM containing 4% PEG and 2% DMSO (Carl Roth) after 24h. 16 to 24 h post-infection, cells
497 were washed twice with PBS and replenished with fresh DMEM supplemented with 2% DMSO.
498 Medium was exchanged every two days until the end of the experiment.

499

500 *Adeno-associated virus (AAV) production and transduction*

501 The hNTCP or CD63 gene was cloned into a self-complementary AAV vector (pscAAV-CMV-
502 EYFP-BGHpolyA⁷⁰). The HB2.7 subgenomic fragment encoding the L-/M-/S-HBsAg of HBV
503 genotype D was cloned into a single-stranded AAV vector (pSSV9-AAV-CMV-EYFP-
504 BGHpolyA)⁷¹. Recombinant AAVs of serotype 6 were produced and iodixanol-purified as
505 described previously⁷². HLCs were transduced with AAVs two days prior to HDV infection (to
506 express NTCP or CD63) or one day after HDV infection (to express HBsAg). 24 h post-
507 transduction, the inoculum was removed, HLCs were washed with DPBS, and replenished with
508 fresh culture medium.

509

510 *Statistics*

511 Graphs and statistical analyses were performed using GraphPad PRISM 8. In all figures
512 where p-values were calculated, the corresponding statistical test is listed in the figure legend.

513

514 For further details regarding the materials and methods used, please refer to supplementary
515 information.

516

517 **Abbreviations**

518 AAV: Adeno-associated virus; ADAR1: adenosine deaminase acting on RNA 1; AFP: 519 alphafetoprotein; ALB: albumin; BLV: Bulevirtide; CHD: chronic hepatitis D; DE: definitive 520 endoderm; DPBS: Dulbecco's phosphate buffered saline; EMA: European Medicines Agency; GT: 521 genotype; HBV: hepatitis B virus; HBc: HBV core antigen; HBsAg: HBV surface protein; HCV: 522 hepatitis C virus; HDV: hepatitis D virus; HDAg: hepatitis delta antigen; hESC: human embryonic 523 stem cell; HEV: hepatitis E virus; HLCs: hepatocyte-like cells; hiPSC: human induced pluripotent 524 stem cell; ISGs: interferon stimulated genes; LNF: Isonafarnib; NTCP: Na^+ -taurocholate co- 525 transporting polypeptide; pegIFN- α : pegylated interferon alpha; PHH: primary human 526 hepatocytes; p.i: post infection; RNP: ribonucleoprotein.

527

528 **Acknowledgements**

529 The authors gratefully acknowledge Dr. John Taylor and Dr. Camille Sureau for generously 530 sharing plasmids. We acknowledge Dr. Vibor Laketa, head of the Infectious Diseases Imaging 531 Platform (IDIP) at the University Hospital Heidelberg for expert support. We thank Andrew 532 Freistaedter and Franziska Schlund for excellent technical support. We thank Dr. Yi Ni for 533 valuable and helpful discussions.

534

535 **Funding**

536 Deutsche Forschungsgemeinschaft (DFG, German Research Foundation) – Projektnummern – 537 272983813 SFB/TRR 179 and 240245660—SFB1129; DZIF - TTU Hepatitis Projects 05.704., 538 05.806., and 05.823; Chica and Heinz Schaller Foundation. JH was supported by a fellowship 539 from the China Scholarship Council.

540

541 **Authors contributions**

542 Conceptualization, H.C., S.U., and V.L.D.T.; Methodology, H.C., and V.L.D.T.; Investigation, H.C., 543 B.Q., A.P., L.M., J.H., R.M.F., F.A.L., Z.Z., and D.G.; Software, H.C.; Data analysis, H.C., B.Q., 544 X.W., D.G., S.U., and V.L.D.T.; Writing-original draft, H.C. and V.L.D.T.; Final draft, H.C., S.U., 545 and V.L.D.T.; Supervision, S.U. and V.L.D.T.; Funding, S.U. and V.L.D.T.

546 **Competing interests**

547 Stephan Urban is co-inventor and applicant on patents protecting HBV preS1-derived lipopeptides 548 (Myrcludex B/Bulevirtide/Hepcludex). All other authors declare no conflict of interest.

549 **Data and materials availability**

550 All data are available in the main text or the supplementary materials.

551

552 **References**

1. Stockdale, A. J. *et al.* The global prevalence of hepatitis D virus infection: Systematic review and meta-analysis. *J. Hepatol.* **73**, 523–532 (2020).
2. Chen, H. Y. *et al.* Prevalence and burden of hepatitis D virus infection in the global population: A systematic review and meta-analysis. *Gut* **68**, 512–521 (2019).
3. Farci, P. & Niro, G. Clinical features of hepatitis D. *Semin. Liver Dis.* **32**, 228–236 (2012).
4. Lempp, F. A. & Urban, S. Hepatitis delta virus: Replication strategy and upcoming therapeutic options for a neglected human pathogen. *Viruses* **9**, 172 (2017).

560 5. Le Gal, F. *et al.* Genetic diversity and worldwide distribution of the deltavirus genus: A study
561 of 2,152 clinical strains. *Hepatology* **66**, 1826–1841 (2017).

562 6. Casey, J. L., Brown, T. L., Colan, E. J., Wignall, F. S. & Gerin, J. L. A genotype of hepatitis
563 D virus that occurs in northern South America. *Proc. Natl. Acad. Sci. U. S. A.* **90**, 9016–
564 9020 (1993).

565 7. Spaan, M. *et al.* Hepatitis delta genotype 5 is associated with favourable disease outcome
566 and better response to treatment compared to genotype 1. *J. Hepatol.* **72**, 1097–1104
567 (2020).

568 8. Hughes, S. A., Wedemeyer, H. & Harrison, P. M. Hepatitis delta virus. *Lancet* **378**, 73–85
569 (2011).

570 9. Lempp, F. A. *et al.* Sodium taurocholate cotransporting polypeptide is the limiting host
571 factor of hepatitis B virus infection in macaque and pig hepatocytes. *Hepatology* **66**, 703–
572 716 (2017).

573 10. Li, H. *et al.* HBV life cycle is restricted in mouse hepatocytes expressing human NTCP. *Cell. Mol. Immunol.* **11**, 175–183 (2014).

574 11. Yan, H. *et al.* Molecular Determinants of Hepatitis B and D Virus Entry Restriction in Mouse
575 Sodium Taurocholate Cotransporting Polypeptide. *J. Virol.* **87**, 7977–7991 (2013).

576 12. Sureau, C. & Negro, F. The hepatitis delta virus: Replication and pathogenesis. *J. Hepatol.*
577 **64**, S102–S116 (2016).

578 13. Kuo, M. Y., Chao, M. & Taylor, J. Initiation of replication of the human hepatitis delta virus
579 genome from cloned DNA: role of delta antigen. *J. Virol.* **63**, 1945–1950 (1989).

580 14. Polson, A. G., Bass, B. L. & Casey, J. L. RNA editing of hepatitis delta virus antigenome
581 by dsRNA- adenosine deaminase Andrew. *Nature* **380**, 454–456 (1996).

582 15. Hwang, S. B. & Lai, M. M. Isoprenylation mediates direct protein-protein interactions
583 between hepatitis large delta antigen and hepatitis B virus surface antigen. *J. Virol.* **67**,
584 7659–7662 (1993).

585 16. Wranke, A., Heidrich, B., Hardtke, S. & Wedemeyer, H. Current Management of HBV/HDV
586 Coinfection and Future Perspectives. *Curr. Hepat. Rep.* **14**, 284–292 (2015).

587 17. Yan, H. *et al.* Sodium taurocholate cotransporting polypeptide is a functional receptor for
588 human hepatitis B and D virus. *Elife* **2012**, 1–28 (2012).

589 18. Jachs, M. *et al.* Response-guided long-term treatment of chronic hepatitis D patients with
590 bulevirtide—results of a “real world” study. *Aliment. Pharmacol. Ther.* **56**, 144–154 (2022).

591 19. Lampertico, P., Roulot, D. & Wedemeyer, H. Bulevirtide with or without pegIFNa for
592 patients with compensated chronic hepatitis delta: From clinical trials to real-world studies.
593 *J. Hepatol.* **77**, 1422–1430 (2022).

594 20. Mascolini, M. Lonafarnib With Ritonavir Slows HDV in 48-Week Placebo Trial. *European
595 Association for the Study of the Liver* (2023).

596 21. Verrier, E. R., Colpitts, C. C., Schuster, C., Zeisel, M. B. & Baumert, T. F. Cell culture
597 models for the investigation of Hepatitis B and D Virus infection. *Viruses* **8**, 1–10 (2016).

598 22. Heuschkel, M. J., Baumert, T. F. & Verrier, E. R. Cell culture models for the study of
599 hepatitis d virus entry and infection. *Viruses* **13**, 1–10 (2021).

600 23. Lempp, F. A. *et al.* Recapitulation of HDV infection in a fully permissive hepatoma cell line
601 allows efficient drug evaluation. *Nat. Commun.* **10**, 1–11 (2019).

602 24. Rodríguez-Antona, C. *et al.* Cytochrome P450 expression in human hepatocytes and
603 hepatoma cell lines: Molecular mechanisms that determine lower expression in cultured
604 cells. *Xenobiotica* **32**, 505–520 (2002).

605 25. Lucifora, J., Michelet, M., Salvetti, A. & Durantel, D. Fast Differentiation of HepaRG Cells
606 Allowing Hepatitis B and Delta Virus Infections. *Cells* **9**, 2288 (2020).

607 26. Jetten, M. J. A., Kleinjans, J. C. S., Claessen, S. M., Chesné, C. & van Delft, J. H. M.
608 Baseline and genotoxic compound induced gene expression profiles in HepG2 and
609 HepaRG compared to primary human hepatocytes. *Toxicol. Vitr.* **27**, 2031–2040 (2013).

610

611 27. Bove, G., Mehnert, A.-K. & Dao Thi, V. L. Chapter 7 - iPSCs for modeling hepatotropic
612 pathogen infections. in *Advances in Stem Cell Biology* (ed. Birbrair, A. B. T. for S. I. D.) vol.
613 8 149–213 (Academic Press, 2021).

614 28. Szkolnicka, D. *et al.* Accurate Prediction of Drug-Induced Liver Injury Using Stem Cell-
615 Derived Populations. *Stem Cells Transl. Med.* **3**, (2014).

616 29. Xia Y, Carpenter A, Cheng X, Block PD, Zhao Y, Zhang Z, Protzer U, L. T. Human stem
617 cell-derived hepatocytes as a model for hepatitis B virus infection, spreading and virus-host
618 interactions. *J. Hepatol.* **66**, 494–503 (2019).

619 30. Wu, X. *et al.* Productive hepatitis C virus infection of stem cell-derived hepatocytes reveals
620 a critical transition to viral permissiveness during differentiation. *PLoS Pathog.* **8**, e1002617
621 (2012).

622 31. Wu, X. *et al.* Pan-Genotype Hepatitis E Virus Replication in Stem Cell-Derived
623 Hepatocellular Systems. *Gastroenterology* **154**, 663–674 (2018).

624 32. Gudima, S., Chang, J., Moraleda, G., Azvolinsky, A. & Taylor, J. Parameters of Human
625 Hepatitis Delta Virus Genome Replication: the Quantity, Quality, and Intracellular
626 Distribution of Viral Proteins and RNA. *J. Virol.* **76**, 3709–3719 (2002).

627 33. Dao Thi, V. L. *et al.* Stem cell-derived polarized hepatocytes. *Nat. Commun.* **11**, 1677
628 (2020).

629 34. Si-Tayeb, K. *et al.* Highly efficient generation of human hepatocyte-like cells from induced
630 pluripotent stem cells. *Hepatology* **51**, 297–305 (2010).

631 35. Zhang, Z. *et al.* Hepatitis D virus replication is sensed by MDA5 and induces IFN- β / λ
632 responses in hepatocytes. *J. Hepatol.* **69**, 25–35 (2018).

633 36. Gudima, S. *et al.* Assembly of Hepatitis Delta Virus: Particle Characterization, Including the
634 Ability To Infect Primary Human Hepatocytes. *J. Virol.* **81**, 3608–3617 (2007).

635 37. Wang, W. *et al.* Assembly and infection efficacy of hepatitis B virus surface protein
636 exchanges in 8 hepatitis D virus genotype isolates. *J. Hepatol.* **75**, 311–323 (2021).

637 38. Freitas, N., Cunha, C., Menne, S. & Gudima, S. O. Envelope Proteins Derived from
638 Naturally Integrated Hepatitis B Virus DNA Support Assembly and Release of Infectious
639 Hepatitis Delta Virus Particles. *J. Virol.* **88**, (2014).

640 39. Tavanez, J. P. *et al.* Hepatitis delta virus ribonucleoproteins shuttle between the nucleus
641 and the cytoplasm. *RNA* **8**, (2002).

642 40. Pollicino, T. *et al.* Replicative and Transcriptional Activities of Hepatitis B Virus in Patients
643 Coinfected with Hepatitis B and Hepatitis Delta Viruses. *J. Virol.* **85**, (2011).

644 41. Zhang, C. *et al.* An RNA Interference/Adeno-Associated Virus Vector-Based
645 Combinatorial Gene Therapy Approach Against Hepatitis E Virus. *Hepatol. Commun.* **6**,
646 878–888 (2022).

647 42. Schulze, A., Gripon, P. & Urban, S. Hepatitis B virus infection initiates with a large surface
648 protein-dependent binding to heparan sulfate proteoglycans. *Hepatology* **46**, (2007).

649 43. Le Seyec, J., Chouteau, P., Cannie, I., Guguen-Guillouzo, C. & Gripon, P. Infection
650 Process of the Hepatitis B Virus Depends on the Presence of a Defined Sequence in the
651 Pre-S1 Domain. *J. Virol.* **73**, 2052–2057 (1999).

652 44. Levy, G. *et al.* Long-term culture and expansion of primary human hepatocytes. *Nat.*
653 *Biotechnol.* **33**, (2015).

654 45. Lange, F. *et al.* Hepatitis D virus infection, innate immune response and antiviral treatments
655 in stem cell-derived hepatocytes. *Liver Int.* 1–14 (2023) doi:10.1111/liv.15655.

656 46. Wu, X. *et al.* Intrinsic Immunity Shapes Viral Resistance of Stem Cells. *Cell* **172**, 423–438
657 (2018).

658 47. Palatini, M. *et al.* IFITM3 Interacts with the HBV/HDV Receptor NTCP and Modulates Virus
659 Entry and Infection. *Viruses* **14**, 727 (2022).

660 48. Macovei, A. *et al.* Hepatitis B Virus Requires Intact Caveolin-1 Function for Productive
661 Infection in HepaRG Cells. *J. Virol.* **84**, 243–253 (2010).

662 49. Iwamoto, M. *et al.* Epidermal growth factor receptor is a host-entry cofactor triggering
663 hepatitis B virus internalization. *Proc. Natl. Acad. Sci. U. S. A.* **116**, 8487–8492 (2019).
664 50. Hinuma, S., Fujita, K. & Kuroda, S. Binding of nanoparticles harboring recombinant large
665 surface protein of hepatitis b virus to scavenger receptor class b type 1. *Viruses* **13**, 1334
666 (2021).
667 51. Li, Y. & Luo, G. Human low-density lipoprotein receptor plays an important role in hepatitis
668 B virus infection. *PLoS Pathog.* **17**, e1009722 (2021).
669 52. Engering, A., Kuhn, L., Fluitsma, D., Hoefsmit, E. & Pieters, J. Differential post-translational
670 modification of CD63 molecules during maturation of human dendritic cells. *Eur. J.
671 Biochem.* **270**, 2412–2420 (2003).
672 53. Carpentier, A., Sheldon, J., Vondran, F. W. R., Brown, R. J. P. & Pietschmann, T. Efficient
673 acute and chronic infection of stem cell-derived hepatocytes by hepatitis C virus. *Gut* **69**,
674 1659–1666 (2020).
675 54. Appelman, M. D., Wettengel, J. M., Protzer, U., Oude Elferink, R. P. J. & van de Graaf, S.
676 F. J. Molecular regulation of the hepatic bile acid uptake transporter and HBV entry receptor
677 NTCP. *Biochim. Biophys. Acta - Mol. Cell Biol. Lipids* **1866**, 158960 (2021).
678 55. Zhang, Z. & Urban, S. New insights into HDV persistence: The role of interferon response
679 and implications for upcoming novel therapies. *J. Hepatol.* **74**, 686–699 (2021).
680 56. Zhang, Z. *et al.* Hepatitis D virus-induced interferon response and administered interferons
681 control cell division-mediated virus spread. *J. Hepatol.* **77**, 957–966 (2022).
682 57. Takayama, K. *et al.* Prediction of interindividual differences in hepatic functions and drug
683 sensitivity by using human iPS-derived hepatocytes. *Proc. Natl. Acad. Sci. U. S. A.* **111**,
684 16772–16777 (2014).
685 58. Greenhough, S., Medine, C. N. & Hay, D. C. Pluripotent stem cell derived hepatocyte like
686 cells and their potential in toxicity screening. *Toxicology* **278**, 250–255 (2010).
687 59. Cayo, M. A. *et al.* A Drug Screen using Human iPSC-Derived Hepatocyte-like Cells
688 Reveals Cardiac Glycosides as a Potential Treatment for Hypercholesterolemia. *Cell Stem
689 Cell* **20**, 478–489 (2017).
690 60. Ninomiya, M. *et al.* The Exosome-Associated Tetraspanin CD63 Contributes to the Efficient
691 Assembly and Infectivity of the Hepatitis B Virus. *Hepatol. Commun.* **5**, 1238–1251 (2021).
692 61. Pols, M. S. & Klumperman, J. Trafficking and function of the tetraspanin CD63.
693 *Experimental Cell Research* vol. 315 1584–1592 (2009).
694 62. Raaben, M. *et al.* NRP2 and CD63 Are Host Factors for Lujo Virus Cell Entry. *Cell Host
695 Microbe* **22**, 688–696 (2017).
696 63. Zona, L. *et al.* CD81-receptor associations - Impact for hepatitis C virus entry and antiviral
697 therapies. *Viruses* vol. 6 875–892 (2014).
698 64. Tanimizu, N. & Miyajima, A. Molecular Mechanism of Liver Development and
699 Regeneration. *International Review of Cytology* vol. 259 1–48 (2007).
700 65. Miyajima, A., Tanaka, M. & Itoh, T. Stem/progenitor cells in liver development,
701 homeostasis, regeneration, and reprogramming. *Cell Stem Cell* vol. 14 561–574 (2014).
702 66. Ni, Y. *et al.* Hepatitis B and D viruses exploit sodium taurocholate co-transporting
703 polypeptide for species-specific entry into hepatocytes. *Gastroenterology* **146**, 1070–1083
704 (2014).
705 67. Dao Thi, V. L. *et al.* Sofosbuvir Inhibits Hepatitis e Virus Replication in Vitro and Results in
706 an Additive Effect When Combined with Ribavirin. *Gastroenterology* **150**, (2016).
707 68. Wettengel, J. M. *et al.* Rapid and robust continuous purification of high-titer hepatitis b virus
708 for in vitro and in vivo applications. *Viruses* **13**, 1503 (2021).
709 69. Sureau, C., Guerra, B. & Lee, H. The middle hepatitis B virus envelope protein is not
710 necessary for infectivity of hepatitis delta virus. *J. Virol.* **68**, 4063–4066 (1994).
711 70. Börner, K. *et al.* Pre-arrayed Pan-AAV Peptide Display Libraries for Rapid Single-Round
712 Screening. *Mol. Ther.* **28**, 1016–1032 (2020).

713 71. Wolff, G. *et al.* Diet-dependent function of the extracellular matrix proteoglycan Lumican in
714 obesity and glucose homeostasis. *Mol. Metab.* **19**, 97–106 (2019).

715 72. Maurer, L. *et al.* Induction of Hepatitis E Virus Anti-ORF3 Antibodies from Systemic
716 Administration of a Muscle-Specific Adeno-Associated Virus (AAV) Vector. *Viruses* **14**, 266
717 (2022).

718 73. Ferns, R. B., Nastouli, E. & Garson, J. A. Quantitation of hepatitis delta virus using a single-
719 step internally controlled real-time RT-qPCR and a full-length genomic RNA calibration
720 standard. *J. Virol. Methods* **179**, 189–194 (2012).

721 74. Spandidos, A., Wang, X., Wang, H. & Seed, B. PrimerBank: A resource of human and
722 mouse PCR primer pairs for gene expression detection and quantification. *Nucleic Acids*
723 *Res.* **38**, D792–D799 (2009).

724 75. Meier, A., Mehrle, S., Weiss, T. S., Mier, W. & Urban, S. Myristoylated PreS1-domain of
725 the hepatitis B virus L-protein mediates specific binding to differentiated hepatocytes.
726 *Hepatology* **58**, 31–42 (2013).

727 76. Stirling, D. R. *et al.* CellProfiler 4: improvements in speed, utility and usability. *BMC*
728 *Bioinformatics* **22**, 1–11 (2021).

729 77. Patro, R., Duggal, G., Love, M. I., Irizarry, R. A. & Kingsford, C. Salmon provides fast and
730 bias-aware quantification of transcript expression. *Nat. Methods* **14**, 417–419 (2017).

731 78. Soneson, C., Love, M. I. & Robinson, M. D. Differential analyses for RNA-seq: transcript-
732 level estimates improve gene-level inferences. *F1000Research* **4**, (2015).

733 79. Love, M. I., Huber, W. & Anders, S. Moderated estimation of fold change and dispersion
734 for RNA-seq data with DESeq2. *Genome Biol.* **15**, 1–21 (2014).

735 80. Alexa, A. & Rahnenfuhrer, J. topGO: enrichment analysis for Gene Ontology. R Packag.
736 version 2.26.0. *R Packag.* version 2.26.0 (2016).

737
738
739
740
741
742
743
744
745
746
747
748
749
750
751
752
753
754
755
756
757
758
759
760
761
762

763 **Tables**

764

765 **Table 1: Primers used in this study**

Name	Sequence (5'-3')	Target	Reference
HDV-F	GCGCCGGCYGGGCAAC	HDV RNA	73
HDV-R	TTCCTCTCGGGTCGGCATG		
HDV-Probe	FAM-CGCGGTCCGACCTGGCATCCG-TAMRA		
RPS11-F	GCCGAGACTATCTGCACTAC	RPS11	33
RPS11-R	ATGTCCAGCCTCAGAACTTC		
NTCP-F	AAGGACAAGGTGCCCTATAAAGG	NTCP	
NTCP-R	TTGAGGACGATCCCTATGGTG		
AFP-F	TGGGACCCGAACTTCCA	AFP	
AFP-R	GGCCACATCCAGGACTAGTTTC		
ALB-F	GGTGTGATTGCCTTGCTC	ALB	
ALB-R	CCCTTCATCCCGAAGTTCAT		
CAV1-F	GCGACCCTAACACCTCAAC	CAV1	74
CAV1-R	ATGCCGTAAAATGTGTGTC		
CAV2-F	AAGACCTGCCTAATGGTTCTGC	CAV2	
CAV2-R	CTCGTACACAATGGAGCAATGAT		
EGFR-F	AGGCACGAGTAACAAGCTCAC	EGFR	
EGFR-R	ATGAGGACATAACCAGCCACC		
LAMP1-F	TCTCAGTGAACTACGACACCA	LAMP1	
LAMP1-R	AGTGTATGTCCTCTCCAAAAGC		
SCARB1-F	CCTATCCCCCTCTATCTCTCCG	SCARB1	
SCARB1-R	GGATGTTGGGCATGACGATGT		
SCARB2-F	AGATGGAGATTCTTTACCCAC	SCARB2	
SCARB2-R	CAGGAACTTATACCGAAAGGCA		
ITGA2-F	CCTACAATGTTGGTCTCCCAGA	ITGA1	
ITGA2-R	AGTAACCAGTTGCCTTTGGATT		
ITGB1-F	CCTACTTCTGCACGATGTGATG	ITGB1	

ITGB1-R	CCTTGCTACGGTTGGTTACATT		
LDLR-F	TCTGCAACATGGCTAGAGACT	LDLR	
LDLR-R	TCCAAGCATTGTTGGTCCC		
CD63-F	CAGTGGTCATCATCGCAGTG	CD63	
CD63-R	ATCGAAGCAGTGTGGTTTT		

766

767

768

769

770

771

772

773

774

775

776

777

778

779

780

781

782

783

784

785

786

787

788

789

790

791

792

793

794

795

796

797

798

799

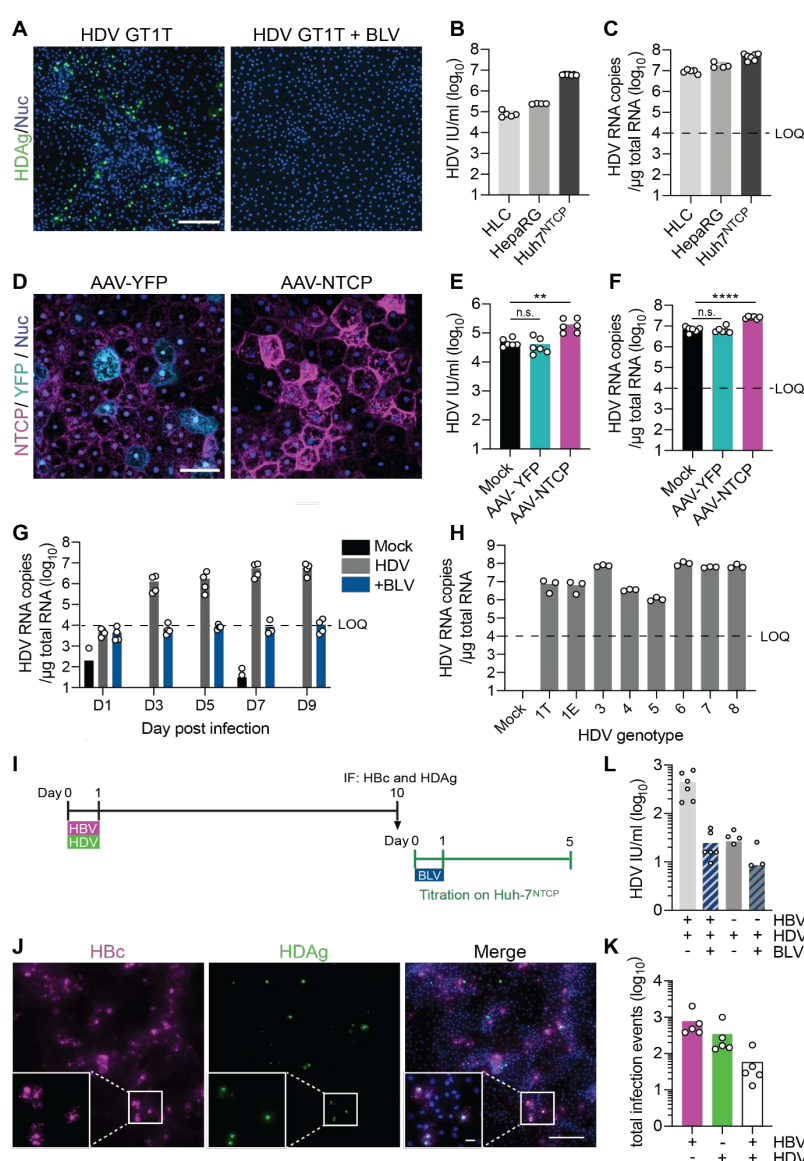
800

801

802

803 **Figures and figure legends**

804



805

806 **Figure 1: Hepatocyte-like cells (HLCs) are susceptible to HDV infection in an NTCP**
807 **dependent manner**

808 (A) HDV infection (MOI = 5) of HLCs incubated with or without 500 nM entry inhibitor bulevirtide (BLV) was
809 assessed by immunofluorescence staining (IF) against the HDV antigen (HDAg, green) five days post-
810 infection (p.i.). Scale bar = 200 μm. (B & C) HLCs, differentiated HepaRG, and Huh7^{NTCP} cells were infected
811 with HDV (MOI = 5). HDV infection was analyzed by (B) counting HDAg-positive cells using CellProfiler or
812 by (C) quantifying HDV genome copies by RT-qPCR. Dashed line: limit of quantification (LOQ); (D) HLCs
813 were transduced with or without AAV (MOI = 10⁴ viral genomes, vg/cell) encoding for YFP or NTCP and
814 stained with Atto-MyrB-565 (magenta) two days later. (E & F) Two days post-transduction, HLCs^{YFP/NTCP}
815 were infected with HDV (MOI = 5 IU/cell) and analyzed by (E) counting HDAg-positive cells or (F)
816 quantifying HDV genome copies five days p.i. Scale bar = 50 μm. Statistical analysis was performed by
817 unpaired two-tailed Student's t test *: p < 0.05; **: p < 0.01; ***: p < 0.001; ****: p < 0.0001; n.s.: non-significant.
818 (G) HDV infection (MOI = 5) of HLCs incubated with or without 500 nM BLV was analyzed by quantifying

819 HDV genome copies in HLC lysates harvested at the indicated days. (H) HLCs were infected with the
820 indicated HDV genotype (MOI = 15 for GTs 1T, 1E, 4, 6, 7, 8; MOI = 30 for GTs 3 & 5) and five days p.i.,
821 HDV genome copies were quantified using RT-qPCR. (I) Experimental setup. HLCs were infected with HBV
822 (MOI = 450 genome copies/cell) and HDV (MOI = 10). (J) Cells were stained against HBV core (HBc,
823 magenta), HDAg (green), and nuclei (DAPI, blue) ten days p.i. Scale bar = 200 μ m, scale bar of insets =
824 40 μ m. (K) HBc- and HDAg-positive cells were counted using ZEN imaging software to quantify HBV and
825 HDV single and co-infection events. Images are representative of three independent differentiations. (L)
826 The supernatant from HBV/HDV- or HDV-infected HLCs collected on day ten p.i. was diluted 1:5 to infect
827 Huh7^{NTCP} cells with or without 500 nM BLV. Infected Huh7^{NTCP} cells were fixed, stained for HDAg, and
828 analyzed using CellProfiler. N = biological replicates.

829

830

831

832

833

834

835

836

837

838

839

840

841

842

843

844

845

846

847

848

849

850

851

852

853

854

855

856

857

858

859

860

861

862

863

864

865

866

867

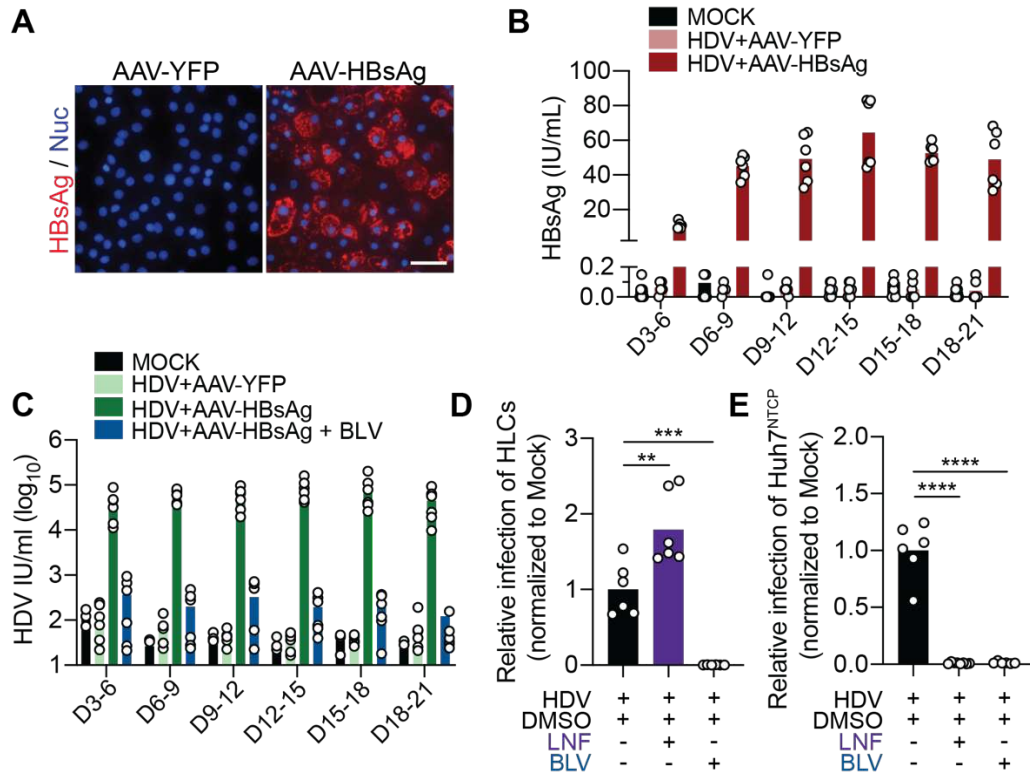


Figure 2: AAV transduction with HBV surface antigens allows completion of the HDV life cycle in HLCs

(A) HLCs were infected with HDV (MOI = 5) and the next day transduced with AAV-YFP or AAV-HBsAg. SN: supernatant. Nine days post-transduction, HLCs were stained for HBsAg (red) and nuclei (blue). Images are representative of two independent differentiations. Scale bars = 50 μ m. (B) HBsAg was quantified in the supernatant by ELISA collected at the end of indicated time periods. (C) Progeny HDV from HLCs harvested at the indicated time points was diluted 1:5 and used to infect Huh7^{NTCP} cells with or without 500 nM BLV. Infected Huh7^{NTCP} cells were fixed and stained for HDAg to quantify HDV infections. (D) HLCs were infected with HDV (MOI = 5), transduced with AAV-HBsAg and incubated with or without 500 nM BLV (between D0-D1 p.i.) or 2 μ M Lonafarnib (LNF; between D0-D5 p.i.). HDV infection was quantified by counting HDAg-positive HLCs five days p.i. (E) The supernatant from these HLCs was diluted 1:5 to infect Huh7^{NTCP} cells which were analyzed for HDV infection by HDAg staining five days p.i. N = biological replicates. Statistical analysis was performed by unpaired two-tailed Student's t test. **: $p < 0.01$; ***: $p < 0.001$; ****: $p < 0.0001$; n.s., non-significant.

868
869

870 **Figure 2: AAV transduction with HBV surface antigens allows completion of the HDV life**
871 **cycle in HLCs**

872 (A) HLCs were infected with HDV (MOI = 5) and the next day transduced with AAV-YFP or AAV-HBsAg.
873 SN: supernatant. Nine days post-transduction, HLCs were stained for HBsAg (red) and nuclei (blue).
874 Images are representative of two independent differentiations. Scale bars = 50 μ m. (B) HBsAg was
875 quantified in the supernatant by ELISA collected at the end of indicated time periods. (C) Progeny HDV
876 from HLCs harvested at the indicated time points was diluted 1:5 and used to infect Huh7^{NTCP} cells with or
877 without 500 nM BLV. Infected Huh7^{NTCP} cells were fixed and stained for HDAg to quantify HDV infections.
878 (D) HLCs were infected with HDV (MOI = 5), transduced with AAV-HBsAg and incubated with or without
879 500 nM BLV (between D0-D1 p.i.) or 2 μ M Lonafarnib (LNF; between D0-D5 p.i.). HDV infection was
880 quantified by counting HDAg-positive HLCs five days p.i. (E) The supernatant from these HLCs was diluted
881 1:5 to infect Huh7^{NTCP} cells which were analyzed for HDV infection by HDAg staining five days p.i. N =
882 biological replicates. Statistical analysis was performed by unpaired two-tailed Student's t test. **: $p < 0.01$;
883 ***: $p < 0.001$; ****: $p < 0.0001$; n.s., non-significant.

884

885

886

887

888

889

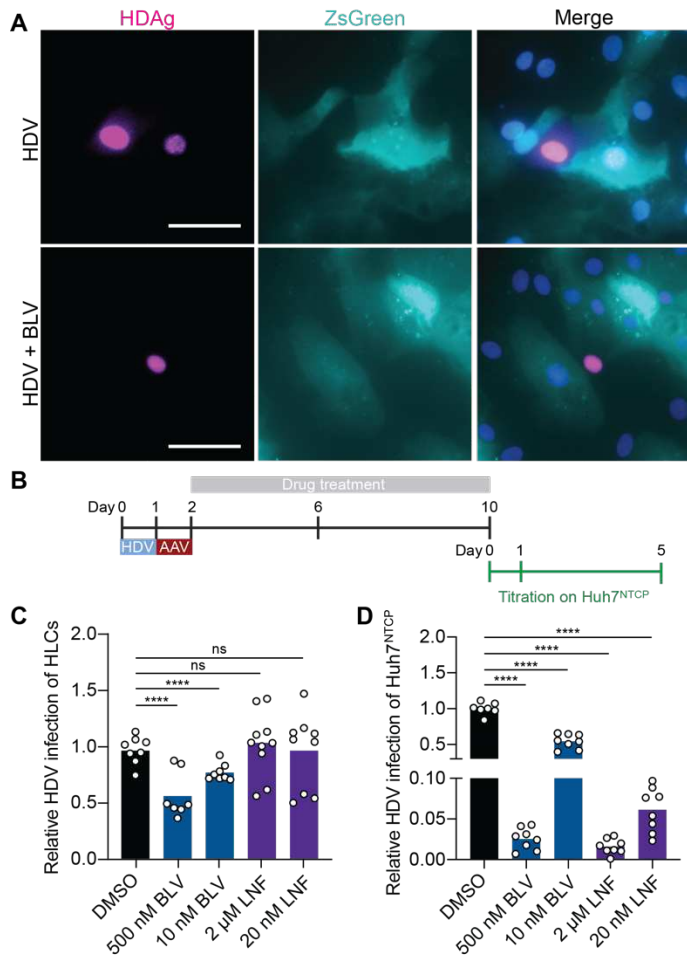
890

891

892

893

894

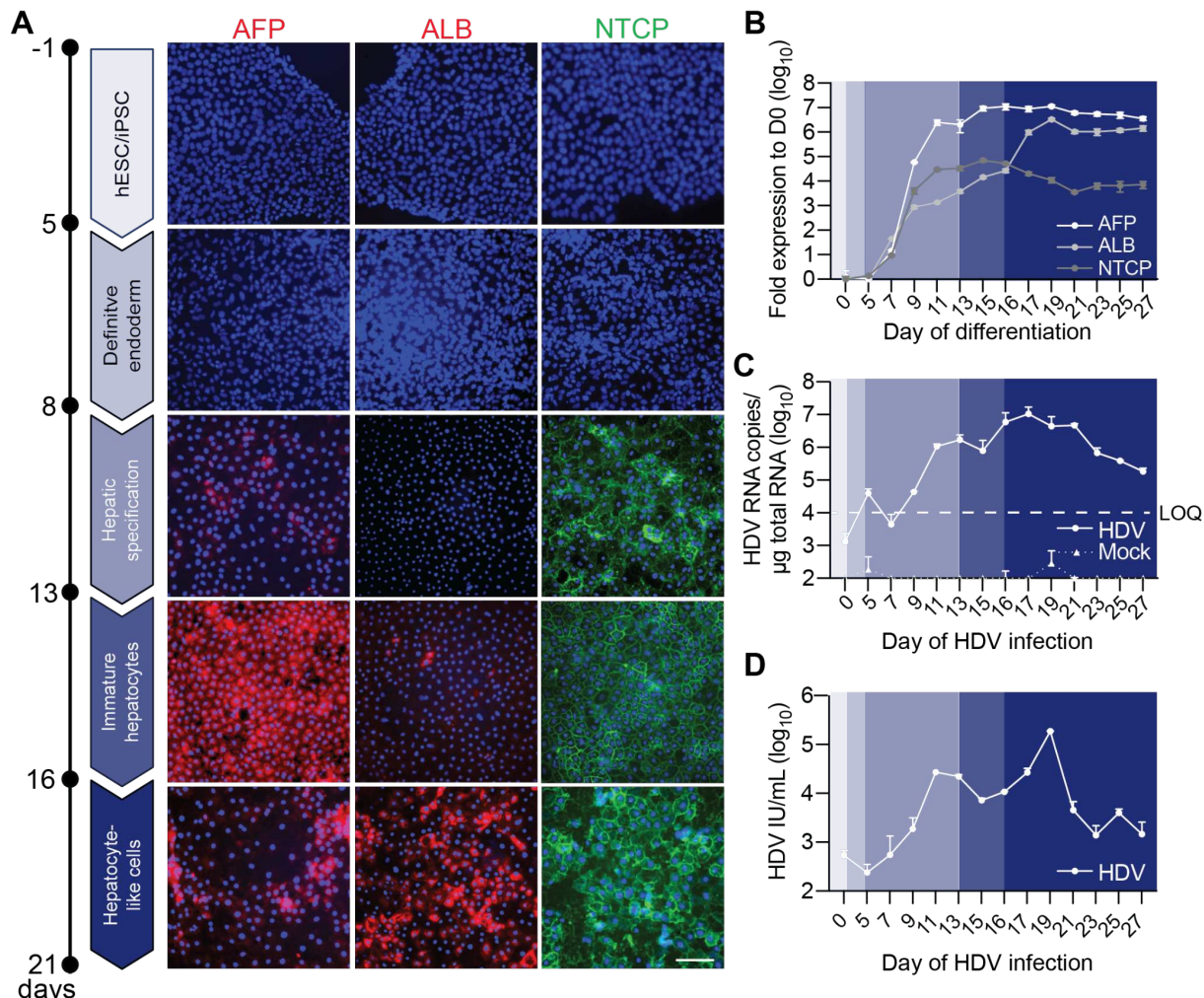


895
896

Figure 3: HDV spread in HBsAg-HLCs allows the evaluation of antiviral HDV regimen

(A) Wild-type HLCs were infected with HDV (MOI = 5) and the next day transduced with AAV-HBsAg. Two days post-infection, they were dissociated and co-cultured with Zs-Green expressing HLCs in the presence or absence of BLV. Eight days later, cells were fixed, stained, and imaged for HDAg (magenta), ZsGreen (cyan) and nuclei (DAPI, blue). Scale bar = 50 μ m (B) Experimental setup. HLCs were infected with HDV (MOI = 5) and the next day transduced with AAV-HBsAg. After removal of the inoculum on day 2 p.i., HLCs were incubated with drugs, which were replenished every four days. Ten days p.i., HLCs were fixed to analyze HDV infections and their culture supernatant harvested for titration of HDV progenies on Huh7^{NTCP} cells. (C) Relative HDV infection events normalized to vehicle DMSO-treated cells were quantified by counting HDAg-positive HLCs 10 days p.i. (D) The supernatant from HLCs was diluted 1:5 to infect Huh7^{NTCP} cells, which were then analyzed for HDV infection by HDAg staining five days p.i. N = biological replicates. Statistical analysis was performed by one-way ANOVA **: $p < 0.01$; ***: $p < 0.001$; ****: $p < 0.0001$; n.s., non-significant.

910
911
912
913
914
915
916



917

Figure 4: HDV susceptibility along stem cell differentiation to hepatocyte-like cells

918 (A) Immunofluorescent images of cells stained against the nuclei (DAPI, blue) and with antibodies against
919 alphafetoprotein (AFP, red), albumin (ALB, red) or Atto-MyrB⁴⁸⁸ (NTCP, green) at the following stages
920 during HLC differentiation: hPSCs, definitive endoderm, hepatic specification, immature, and mature
921 hepatocyte-like cells. Images are representative of two independent differentiations. Scale bar = 100 μm .
922 (B) Cells were harvested for analyzing ALB, AFP, NTCP expression using RT-qPCR at the indicated day
923 of the differentiation protocol. (C & D) Cells were infected with HDV at the indicated day of the differentiation
924 protocol and harvested five days p.i. HDV infection was analyzed by quantifying (C) HDV genome copies
925 and (D) HDAg-positive cells using CellProfiler. Dashed line: LOQ. Results represent the mean \pm SD of N =
926 2.
927

928

929

930

931

932

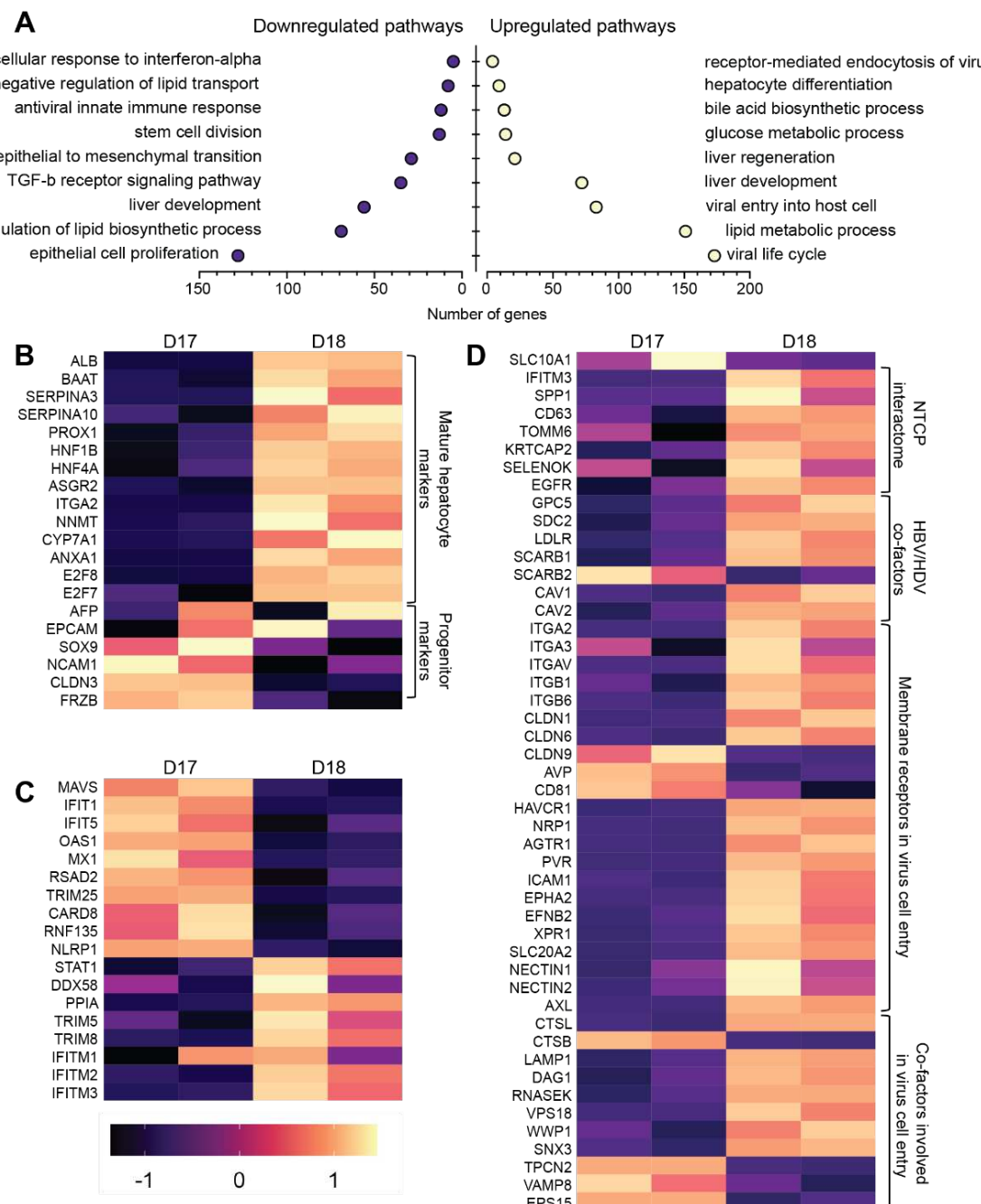
933

934

935

936

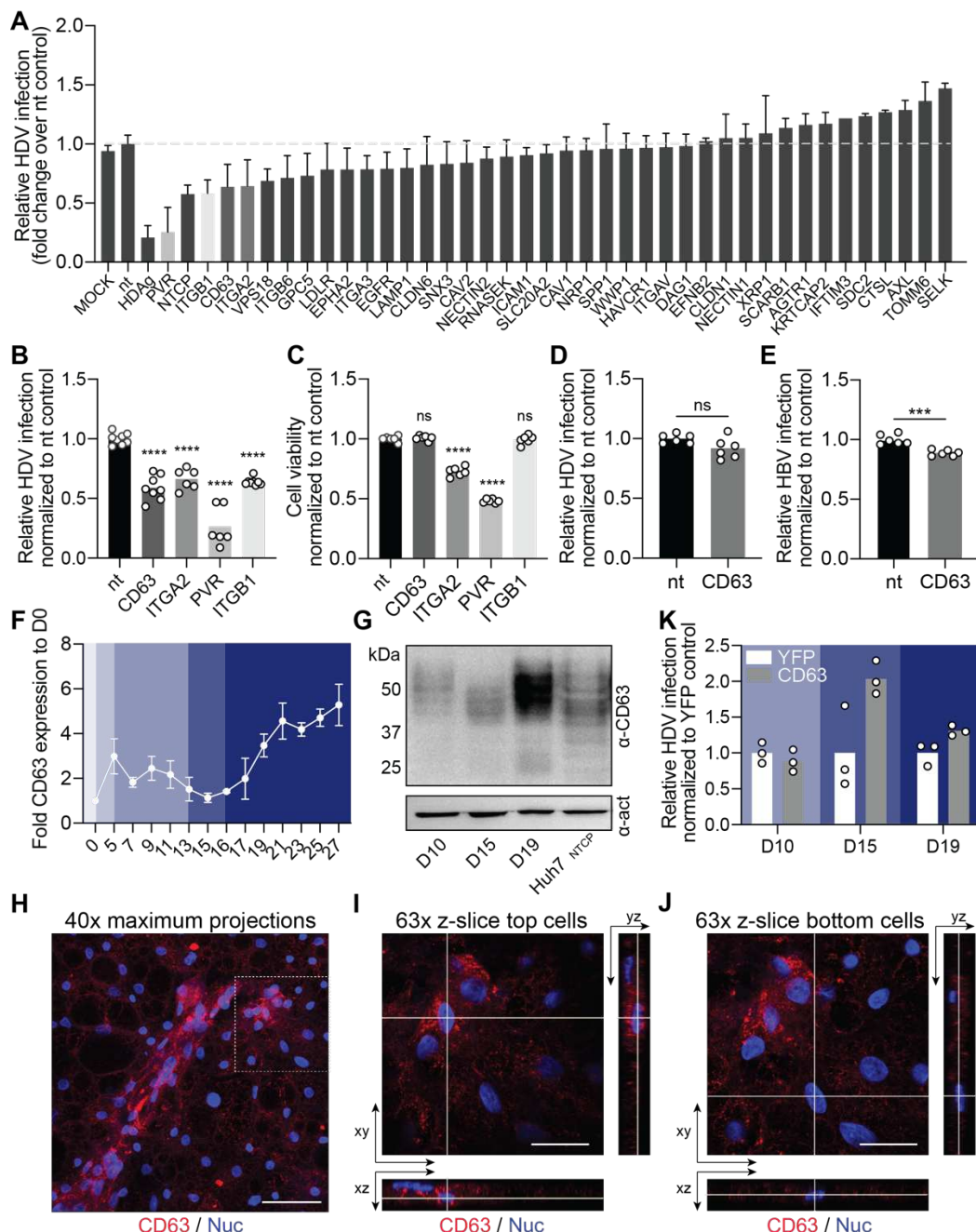
937



938

939 **Figure 5: Differential gene expression analysis reveals upregulation of HBV/HDV entry**
 940 **factors in mature HLCs.**

941 Total RNA was extracted from HLCs at either day 17 or 18 during the differentiation protocol and subjected
 942 to whole-transcriptome expression profiling and gene ontology (GO) term enrichment analysis. (A) GO term
 943 enrichment analysis of biological pathways for up- and down-regulated genes between HLCs at day 17 and
 944 18. Differentially expressed genes (p value <0.05) were significantly enriched in this GO term. (B-D)
 945 Heatmap of Z score-normalized counts per million (CPM) values for (B) hepatocyte markers, (C) innate
 946 immune genes, and (D) virus entry factors. N = biological replicates.



947
948

Figure 6: siRNA screen reveals CD63 to be potential co-factor of HBV/HDV entry which could be rate-limiting for infection of immature hepatocytes.

951 (A) siRNA screen of potential HDV host factors. Huh7^{NTCP} cells were transfected with 50 nM on-target pool
952 siRNAs directed against indicated genes and 24 h later infected with HDV (MOI = 1). Relative HDV infection
953 was normalized to non-target (nt) siRNA transfection and quantified by counting HDAg-positive cells five
954 days p.i. (B & C) Four genes were selected and confirmed by separate siRNA transfection into Huh7^{NTCP}
955 cells and analyzed for (B) HDV infection and (C) cell toxicity. Statistical analysis was performed by one-
956 way ANOVA **: $p < 0.01$; ***: $p < 0.001$; ****: $p < 0.0001$; n.s., non-significant. (D) Huh7^{NTCP} cells were infected
957 with HDV (MOI = 1) and 24 h later transfected with nt- and CD63-siRNAs. HDV infections were quantified
958 by counting HDAg-positive cells five days p.i. Statistical analysis was performed by unpaired two-tailed

959 Student's t test. **: $p <0.01$; ***: $p<0.001$; ****: $p<0.0001$; n.s., non-significant. (E) HepG2^{NTCP} cells were
960 transfected with nt- and CD63-siRNAs and 48 h later, infected with HBV (MOI = 300 genome copies/cell).
961 HBV infections were quantified by counting HBV core-positive cells 10 days p.i. Statistical analysis was
962 performed by unpaired two-tailed Student's t test. **: $p <0.01$; ***: $p<0.001$; ****: $p<0.0001$; n.s., non-
963 significant. (F) HLCs were harvested for analyzing CD63 expression using RT-qPCR at the indicated day
964 of the differentiation protocol. (G) Western blot analysis of Huh7^{NTCP} cells as control and HLC cell lysates
965 harvested at indicated day of the differentiation protocol, for CD63 and β -actin (act) expression using
966 respective antibodies. (H-I) HLCs at their fully matured stage were fixed, stained for CD63 (red) and the
967 nucleus (blue) and imaged at the Airyscan confocal microscope. (H) Maximum intensity projections on 40x
968 tile image stacks showing both, top and bottom HLCs. Scale bar = 50 μ M. Single z-slice and orthogonal xz
969 and yz views of (I) top HLCs or (J) bottom HLCs. Scale bar = 20 μ M. (K) Cells at indicated day of the
970 differentiation protocol were transduced with AAV-YFP or AAV-CD63 and two days later, infected with HDV.
971 Relative HDV infections were quantified by counting HDAg-positive cells five days p.i. N = biological
972 replicates.